PAPER

Structural changes in the crystal lattice in enamel under Er,Cr:YSGG laser irradiation and oven heated by Rietveld analysis

IOP Publishing | Astro Ltd Laser Physics

Laser Phys. **34** (2024) 015601 (8pp) https://doi.org/10.1088/1555-6611/ad0cb2

Structural changes in the crystal lattice in enamel under Er,Cr:YSGG laser irradiation and oven heated by Rietveld analysis

J S Rabelo Neto[1,*], P A da Ana[2], V L Mazzocchi[3], M E G Valério[4] and D M Zezell[5,*]

[1] Mechanical Engineering Department, University of Aveiro, Aveiro, Portugal
[2] Center for Engineering, Modeling, and Applied Social Sciences, Federal University of ABC, São Bernardo do Campo, Brazil
[3] Research Reactor Center, Institute of Energy and Nuclear Research, São Paulo, Brazil
[4] Laboratory of Preparation and Characterization of Materials, Physics Department, Federal University of Sergipe, Sergipe, Brazil
[5] Center for Lasers and Application, Institute of Energy and Nuclear Research, São Paulo, Brazil

E-mail: joserabelo@ua.pt and zezell@usp.br

Received 20 September 2023
Accepted for publication 1 November 2023
Published 4 December 2023

Abstract

Changes in the crystal lattices and compositions of the dental enamel powders were evaluated after oven or Er,Cr:YSGG laser irradiation. A decrease in the Ca/P ratio to levels close to the ideal theoretical value of laser irradiation caused a considerable decrease in the hydroxyapatite crystallite size but without changes in the crystallographic phase. These changes alter the material, can affect the demineralization process, and are useful for the prevention of caries and dental erosion.

Keywords: laser ablation, dentistry, thermal effects

1. Introduction

The application of lasers in dentistry has spread rapidly over the past few years across various specialties. In the case of dental caries, high-powered lasers have been used mainly for the removal of caries by ablation [1–9]. The use of lasers to prevent dental caries has been studied through the use of laser irradiation on parameters that cause chemical and physical changes, without the need for ablated tissue, so that this material has a greater resistance to demineralization [10–17]. In recent years, several studies have sought to answer important questions regarding laser action in caries prevention, strengthening enamel demineralization, the effect of material ablation, and effects that can alter the structure of materials [18–22].

The mineral matrix of both enamel and dentin is composed of hydroxyapatite $[Ca_{10}(PO_4)_6(OH)_2]$ (HAP)-carbonated. This matrix contains HAP crystals with carbonate radicals that partially replace the phosphate radicals and hydroxyl [23, 24]. The apatite mineral family $[A_{10}(BO_4)_6X_2]$ is crystallized in hexagonal prisms, where A is usually Ca^{2+} or Pb^{2+}, B is P^{5+} or As^{5+}, and X is F^-, Cl^-, or $(OH)^-$ [25, 26]. The unit cell dimensions are $a = b = 9.4343$ Å, $c = 6.8681$ Å, and $V = 529.3$ Å [27]. The mineral parts of bones and teeth are an impure form of HAP, with a variable composition of Ca/P ranging from 1.6 to 1.7 [28].

The chemical changes associated with the process of tooth decay include: (a) decreased bone mineral density, (b)

* Authors to whom any correspondence should be addressed.

decreased Ca/P and crystallographic changes including: (a) increased *a*-axis in the region of caries compared to other regions in the enamel, and (b) presence of larger crystals of apatite. The incorporation of HPO_2^{-4}, which can cause expansion of the *a*-axis and large crystals, may be related to the decrease in carbonate CO_2^{-3} [23].

Er,Cr:YSGG laser with a wavelength of 2.79 μm, has also been studied for caries prevention. Previous studies have reported a significant decrease in enamel resistance to demineralization after Er,Cr:YSGG laser irradiation [7, 29, 30], suggesting its cariostatic potential, and this effect could be due to the heating [31] of the crystalline lattice of HAP [32, 33].

This study evaluates the changes induced in the crystal lattice of HAP under the action of a heating furnace and laser irradiation of Er,Cr:YSGG. Attempts to understand possible explanations for why certain changes in the crystal lattice of HAPs can cause changes in their properties are mainly related to their resistance to dissolution.

2. Materials and methods

2.1. Preparation of enamel powder oven-heated

Enamel slices were obtained from bovine incisor teeth by sagittal sectioning, after which the backside of the slices was grounded to remove all dentin remnants. The slices were then triturated in a mortar until a powder was formed. Four samples of 1 g of enamel powder were heated in an oven at a rate of 10 °C min to 200 °C, 600 °C, 800 °C, and 1000 °C, for 1 h. Three pellets were prepared for each sample by pressing 5 mg of each sample with 100 mg of KBr with 4 tons during 10 min.

2.2. Preparation of enamel powder under laser ablation

The enamel powder was obtained as previously described. Three pellets were prepared with 0.4 g of enamel powder and were irradiated with an Er,Cr:YSGG laser (Millennium, Biolase Inc., San Clemente, USA) that operates at a wavelength of 2.79 μm, pulse width of 140–200 us, and repetition rate of 20 Hz. It used a G-6 mm tip (beam diameter of 600 μm) was used, and the energy per pulse was measured five times using a power/energy meter (Fieldmaster-Coherent, Santa Clara, USA) before laser irradiation. The irradiation conditions are listed in table 1.

2.3. Temperature measurements during laser irradiation

This study used energy densities near or below the ablation threshold for enamel as reported in the literature [34–36]. The surface temperature of the enamel slices during laser irradiation was measured using an infrared thermographic camera (ThermaCam FLIR SC3000 Systems, Boston, USA). This camera is equipped with a quantum well infrared photodetector cooled to 70 °C, capable of recording temperatures in the range of 20 °C–1500 °C, with a resolution of 0.01 °C, a response time of 0.02 s an acquisition rate of 60 Hz. During the experiments, the temperature was controlled at 21.4 °C and the room humidity was 36%. The experiments were conducted on enamel slices using a lens with a focal length of 0.1 m. Data were analyzed using dedicated software (ThermaCam Research 2001, Boston, USA).

Table 1. Laser irradiation conditions of the enamel samples.

Group	$E_{\text{mean/pulse}}$, mJ	Energy density, J cm^{-2}
1	21.30 ± 0.42	7.53 ± 0.15
2	38.84 ± 0.77	13.74 ± 0.27

2.4. X-ray diffraction

Powdered enamel oven samples overheated and ablated by laser irradiation were subjected to x-ray diffraction (XRD) analysis at the Laboratory of Synchrotron Light (LNLS) in line D12A-XRD1. The powder station was the x-ray K of Cu with =0.1541 nm, which was scanned from 20° to 60°, with steps of 0.02°, keeping constant energy for each point collected. The samples were sieved and placed in a capillary with a diameter of 5 mm by adjusting the capillary in the equipment to turn itself around its own axis.

The Rietveld method [37] allows the simultaneous refinement of the unit cell, refinement of the crystal structure, microstructure analysis, quantitative analysis of phases, and determination of the preferred orientation from the diffraction data of x-rays or neutrons. In this study, it was used primarily to confirm the crystallographic phases present in the samples, previously identified by analysis of the positions of peaks in the diffraction of x-rays of each sample using the GSAS software [38]. HAP (PDF 09-0432), octacalcium phosphate (OCP) (PDF 26-1056), tricalcium phosphate phase β (β-TCP) (PDF 09-0169), tetracalcium phosphate (TTCP) (PDF 25-1137), tricalcium phosphate phase α (PDF 09-0348), calcium oxide (PDF 07-5785), calcium carbonate (PDF 01-5194), dicalcium phosphate (PDF 03-1046) and dicalcium phosphate dihydrate (PDF 01-6132). The diffraction pattern of silicon [Standard Reference Materials National Institute of Standards and Technology (NIST) SRM-640c] was used to analyze the instrumental data of our experiments. The results obtained with the Rietveld method, in addition to proof of the phases in the samples and taking of their proportions, we obtained the sizes of the *a*-axis, *c*-axis, unit cell volume, crystallite size, and occupancy rates of the atoms of calcium and phosphorus in the crystallographic structure.

3. Results

The infrared thermography showed a surface temperature of 350 °C for laser irradiation at 7.53 J cm^{-2} and 600 °C for 13.74 J cm^{-2}. Enamel samples were heated in an oven at temperatures of 200 °C–600 °C there was no crystallographic phase change, confirming the presence of 100% HAP matching pattern PDF 09-0432.

Table 2 shows the Rietveld results for the enamel samples heated in an oven and natural enamel. Only the samples heated to 800 °C, in addition to HAP, showed stages of OCP with code PDF 26-1056 and β-TCP with code (PDF 09-0169), with

Table 2. Rietveld results for heated in-oven enamel samples.

	Enamel	Enamel (200 °C)	Enamel (600 °C)	Enamel (800 °C)
		Lattice		
$a = b$	9.45 ± 0.0007 Å	9.44 ± 0.003 Å	9.44 ± 0.001 Å	9.44 ± 0.0009 Å
c	6.89 ± 0.0005 Å	6.88 ± 0.002 Å	6.88 ± 0.001 Å	6.88 ± 0.0006 Å
		Cell volume		
V (Å^3)	533.4 ± 0.1 Å^3	531.3 ± 0.4 Å^3	530.7 ± 0.2 Å^3	531.4 ± 0.1 Å^3
		Occupation		
Ca_1	0.9670	0.9572	0.9805	0.9390
Ca_2	0.9061	0.9302	0.9698	0.9503
P	0.8929	0.9159	0.9434	0.9143
		Ca/P		
Ca/P	1.74	1.71	1.72	1.72
		Crystallites		
(nm)	29.2 ± 0.4	21.8 ± 0.3	26.4 ± 0.3	29.5 ± 0.4
R_p (%)	8.21	7.65	7.47	8.95
R_{wp} (%)	10.31	9.77	9.47	11.53
χ^2	1.34	1.15	1.26	1.52

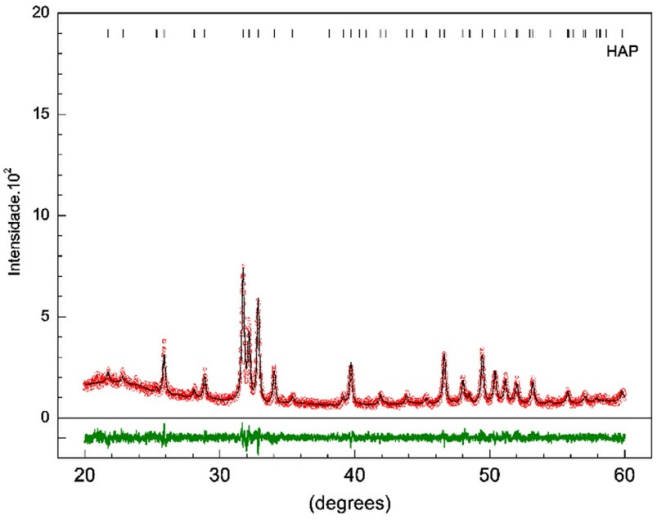

Figure 1. The pattern observed (O) versus the calculated (▬) in the enamel sample heated at 200 °C and the index (▮) of the standard reflections that contribute to the sample diffractogram.

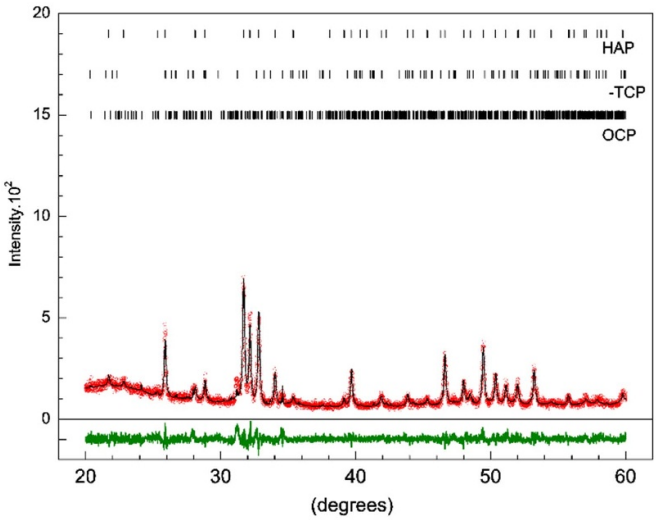

Figure 2. The pattern observed (O) versus the calculated (▬) in the enamel sample heated at 800 °C and the index (▮) of the standard reflections that contribute to the sample diffractogram.

ratios of 4.40% and 1.53%, respectively. Figures 1 and 2 show the calculated and observed diffraction patterns for enamel samples heated to 200 °C and 800 °C, respectively.

The table 3 shows the results of Rietveld analysis of laser-irradiated enamel samples. The enamel samples irradiated with energy densities of 7.53 ± 0.15 J cm^{-2} and 13.74 ± 0.27 J cm^{-2}, did not observe any change of crystallographic phase being validated the presence of 100% HAP corresponding to the standard PDF 09-0432. Figure 3 shows a graphical representation of the Rietveld results for the enamel sample irradiated at 7.53 J cm^{-2}.

Figures 4–7 show the variations in the values of axis-*a*, axis-*c*, unit cell volume, and crystallite size of the HAP, respectively, based on the Rietveld method of the heated and irradiated XRD enamel samples. In the figures, the density measurements of the laser energy are correlated with the surface temperatures during irradiation.

The enamel samples irradiated with energy densities of 7.53 ± 0.15 J cm^{-2} and 13.74 ± 0.27 J cm^{-2}, did not observe any change of crystallographic phase being validated the presence of 100% HAP corresponding to the standard PDF 09–0432. Figure 3 shows a graphical

Table 3. Results obtained by Rietveld analysis of laser-irradiated enamel samples.

	Enamel	Enamel (7.53 J cm^{-2})	Enamel (13.74 J cm^{-2})
		Lattice	
$a = b$	9.4547 ± 0.0007 Å	9.447 ± 0.002 Å	9.441 ± 0.002 Å
c	6.8911 ± 0.0005 Å	6.886 ± 0.002 Å	6.885 ± 0.001 Å
		Cell volume	
V (Å^3)	533.4 ± 0.1 Å^3	532.2 ± 0.4 Å^3	532.5 ± 0.3 Å^3
		Occupation	
Ca_1	0.9670	0.9869	0.9798
Ca_2	0.9061	0.9528	0.9612
P	0.8929	0.9578	0.9592
		Ca/P	
Ca/P	1.736	1.6917	1.6831
		Crystallites	
(nm)	29.2 ± 0.4	26.1 ± 0.2	25.4 ± 0.2
R_p (%)	8.21	6.36	7.00
R_{wp} (%)	10.31	8.16	8.94
χ^2	1.34	1.19	1.33

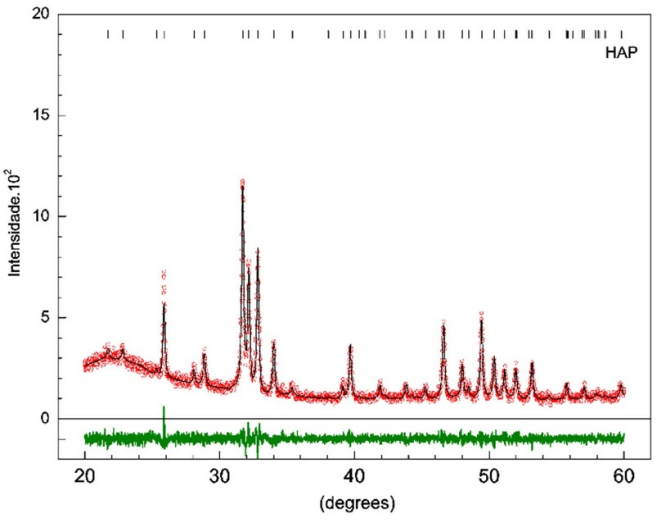

Figure 3. The pattern observed (○) versus the calculated (▬) in the enamel sample irradiation at 7.53 J cm^{-2} and the index (▮) of the standard reflections used in the Rietveld method that influences the sample diffraction.

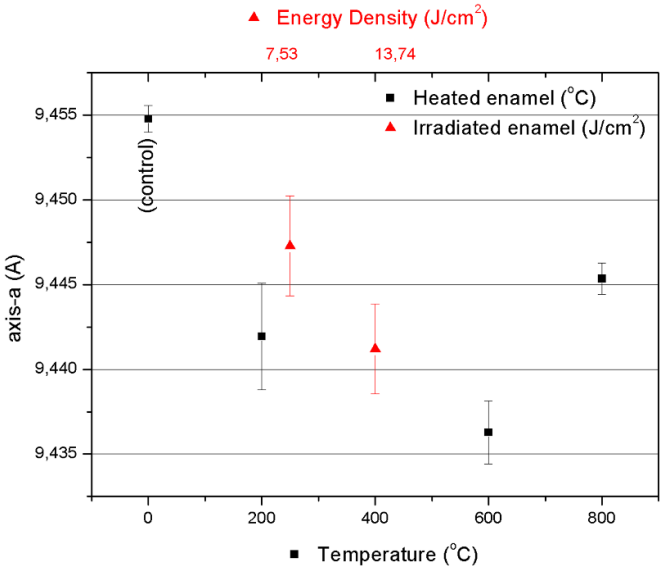

Figure 4. Variations in the a-axis for heated and irradiated enamel samples.

representation of the Rietveld results for the enamel sample irradiated at 7.53 J cm^{-2}. Figures 4–7 show the variations in the values of axis-a, axis-c, unit cell volume, and crystallite size of the HAP, respectively, based on the Rietveld method of the heated and irradiated XRD enamel samples. In the figures, the density measurements of the laser energy are correlated with the surface temperatures during irradiation.

In the present study regarding the appearance of new crystallographic phases in the material subjected to laser irradiation and heated in an oven, analyses by XRD and by the Rietveld method showed that both enamel types had a certain resistance to phase change at 800 °C and should be made only by the HAP phase.

The behavior of HAP under the temperature effect has been reported in the literature, where it was found that the material begins to decompose at 700 °C, for carbonate removal in the system [39]. In the phase transformations of HAP between 25 °C and 500 °C, the material shows diffraction patterns with the same HAP reflection [40]. The HAP is stable until

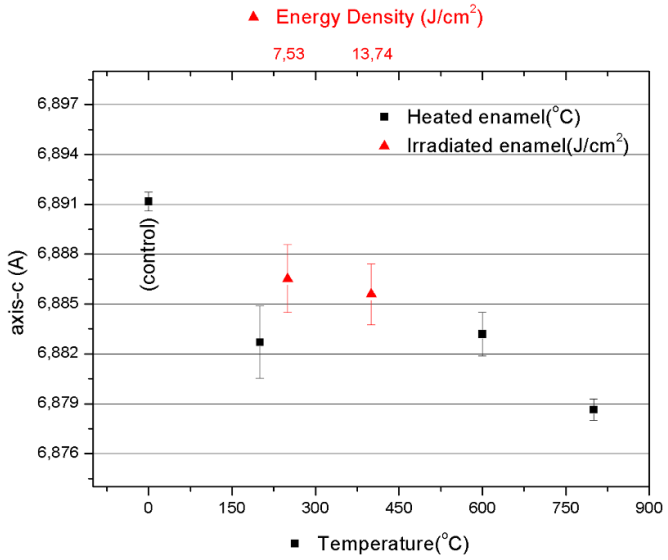

Figure 5. Variations in axis *c* for heated and irradiated enamel samples.

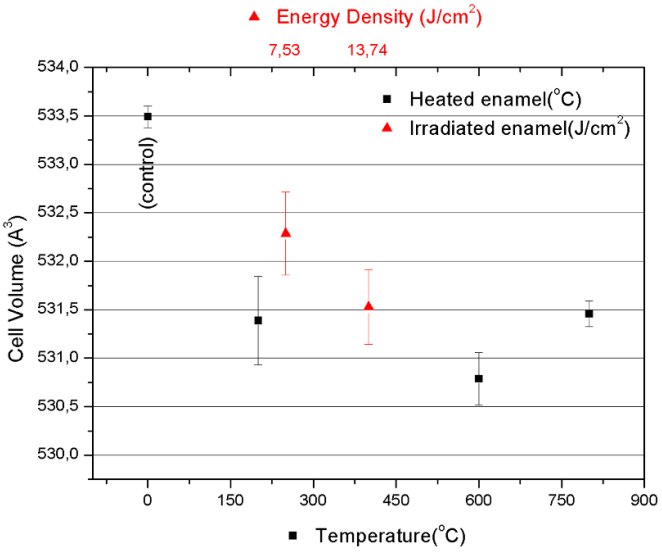

Figure 6. Variations in unit cell volume of heated and irradiated enamel samples.

the temperature reaches 600 °C, after which dehydroxylation occurs up to ∼1200 °C and β-TCP [$Ca_3(PO_4)_2$] and TTCP [$Ca_4O(PO_4)_2$] are formed [41]. Presence is the onset of β-TCP [$Ca_3(PO_4)_2$] in a heating duration of 1 h at 10 °C–800 °C, ranging from 10% to 20% of this phase in the material [42]. Our analysis found OCP and TCP phases in enamel heated at 800 °C for 1 h.

The behavior of HAP under the temperature effect has been reported in the literature, where it was found that the material begins to decompose at 700 °C, for carbonate removal in the system [39]. In the phase transformations of HAP between 25 °C and 500 °C, the material shows diffraction patterns with the same HAP reflection [40]. The HAP is stable until the temperature reaches 600 °C, after which dehydroxylation occurs up to ∼1200 °C and β-TCP [$Ca_3(PO_4)_2$] and TTCP [$Ca_4O(PO_4)_2$] are formed [41]. Presence is the onset of β-TCP [$Ca_3(PO_4)_2$] in a heating duration of 1 h at 10 °C–800 °C, ranging from 10% to 20% of this phase in the material [42]. Our analysis found OCP and TCP phases in enamel heated at 800 °C for 1 h.

Even with only the HAP phase, the material can change its structure, such as the amount of carbonate, which can cause changes in the resistance properties to HAP degradation. Another factor that may influence material solubility is the crystallite size. Among the samples that showed evidence of HAP single phase, for the Rietveld method, we found structural differences within this phase that are important to understand the different behaviors in their properties without even changing the material to another crystallographic phase.

Regarding the variation of the *a*-axis (figure 4) unit cell of HAP in enamel, we found that heating up the action level of 600 °C and irradiation resulted in a reduction of this axis, and above this temperature, growth. This effect has been reported by other authors, which took place under thermal action until the temperature reached 400 °C and grew after this temperature [24].

It is believed that this variation is caused by the presence of $HAPO_2^{-4}$ reacting with CO_2^{-3} in temperatures above 300 °C, the increase in *a*-axis above 400 °C is due to the loss of CO_2^{-3} type B and changing the replacement of carbonate type B by the type A at high temperatures. The enamel samples also showed a decrease in the *c*-axis, but to a lesser degree (figure 5), with increasing temperature, and this effect was not reversed. The variation in the *a*-axis size and *c*-axis reflected the dimensions of the unit cell volume (figure 6). There was a decrease in the unit cell volume to the limit of 600 °C and a small increase above this temperature. These effects are mainly influenced by the *a*-axis. The unit-cell volume behavior is reflected in the crystallite size (figure 7), which decreases until the temperature reaches 600 °C and subsequently increases. This behavior was also observed in enamel samples irradiated by the laser.

In the studies reported by dependency analysis on the dissolution properties of sparingly soluble minerals, HAP has been observed to be dependent on the crystallite size, and if these crystallites are on the nanometer scale, the dissolution of the material cannot be interpreted in terms of conventional theories developed for studies on microcrystals. The authors found that the dissolution can be self-inhibited or even suppressed owing to the crystallite decrease in nanometric-scale conditions [43].

In another study, it was reported that HAP nanostructure crystallites with an average size of 20 nm were insensitive to dissolution, where one layer of HAP nanoparticles was deposited on the enamel surface, protecting it significantly under acidic conditions, which was considered surprising by the authors [44]. In our study, we found crystallite sizes on the nanoscale, which varied from 20 to 30 nm. The Ca/P HAP is important for evaluating the distribution of calcium and phosphorus in the structure, where the ideal is 1.67 [41, 45–48] and the reference standard NIST presents a value of Ca/P = 1.664 ± 0.005 [49].

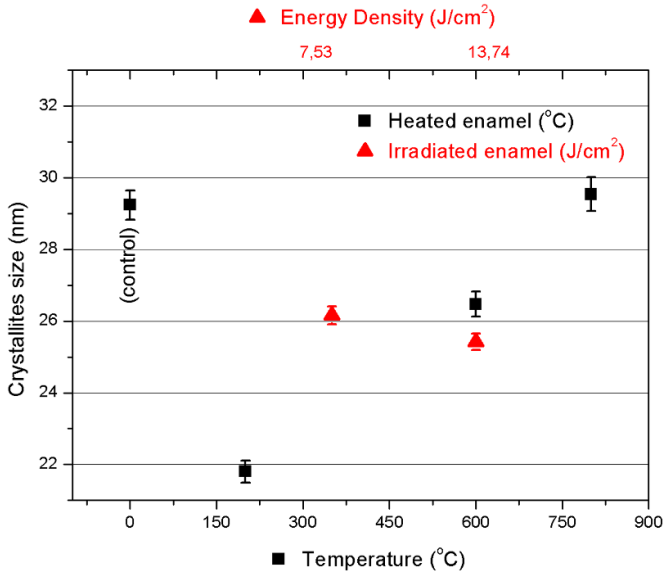

Figure 7. Variation in crystallite size of heated and irradiated enamel samples.

Changes in this relationship have been due to materials deficient in calcium or even in excess, which can cause different behaviors in the material properties. Observed in our study that the samples showed a calcium excess in the structure, but with the temperature increase in the oven and also the laser irradiation, this ratio decreased, approaching the ideal ratio of 1.67. The relationship between the laser irradiation on enamel samples and the effect of making the material came very close to the ideal ratio of 1.67 on the crystallographic structure of HAP's.

Enamel samples irradiated at 7.53 J cm^{-2} and 13.74 J cm^{-2} occur Ca/P 1.6817 and 1.6831, respectively. In a recent study that evaluated the Ca/P variation in enamel under laser irradiation of Er,Cr:YSGG of premolar teeth surface with irradiation of 17.68 J cm^{-2} and 35.36 J cm^{-2} no change occurred in the Ca/P ratio [50]. However, this study has been used in the system to spray water during irradiation, which causes an increase in the ablative effect, expelling the material that was exposed to the laser beam more effectively, resulting in surface cleaning of the area that was influenced by the laser.

Erkmen Almaz *et al* [51] argue that the Er,Cr:YSGG laser irradiation may influence the prevention of teeth enamel demineralization considering the increase in the temperature. Alkhudhairy *et al* [52] emphasized that the Er,Cr:YSGG laser may remove minimal material and cause potential thermomechanical damage by ablation, but the increased temperature may eliminate free radicals and improve the bond strength of the enamel. Ulusoy *et al* [53] argued that Er,Cr:YSGG laser application without water cooling increases enamel resistance to demineralization. Benetti *et al* [54] emphasized that the Er,Cr:YSGG laser irradiated under similar energy densities used in this study promotes changes in bone tissues, whether in mineral or organic material, specifically in carbonate content, and argued that it is important to choose the correct energy density in clinical procedures to minimize thermal damage and stimulate the best healing.

4. Conclusion

Both oven heating and laser irradiation resulted in a decrease in the HAP crystallite sizes and enamel, maintaining the HAP crystallographic phase. Laser irradiation resulted in an improvement in the Ca/P ratio, bringing it closer to the ideal ratio of 1.67. These changes are important because they can make enamel more resistant to demineralization.

Acknowledgments

This work was supported by the Brazilian Synchrotron Light Laboratory (LNLS) proposal D12A-XRD1 7760, FAPESP/CEPID (05/51689-2), CAPES/Procad (0349/05-4), and Rede de Nanofotônica—MCT/CNPq (555170/2005-5).

Conflict of interest

The authors declare that they have no conflicts of interest to disclose regarding the submission of this article.

ORCID iDs

J S Rabelo Neto https://orcid.org/0000-0002-9769-5675
P A da Ana https://orcid.org/0000-0003-2857-7517
V L Mazzocchi https://orcid.org/0659-7015-6707-7923
M E G Valério https://orcid.org/0000-0003-1707-1078
D M Zezell https://orcid.org/0000-0001-7404-9606

References

[1] Rechmann P and Hennig T 2001 Lasers in periodontology today and tomorrow *Med. Laser Appl.* **16** 223–30
[2] Serdar-Eymirli P, Turgut M D, Dolgun A and Yazici A R 2019 Effect of Er,Cr:YSGG laser, fluoride, and CPP-ACP on caries resistance in primary enamel *Lasers Med. Sci.* **34** 881–91
[3] Coluzzi D J 2003 Lasers in dentistry—wonderful instruments or expensive toys *Int. Congr. Ser.* **1248** 83–90
[4] Hibst R and Keller U 1989 Experimental studies of the application of the Er:YAG laser on dental hard substances I *Lasers Surg. Med.* **9** 338–44
[5] Hibst R and Keller U 1989 Experimental studies of the application of the Er:YAG laser on dental substances, II *Lasers Surg. Med.* **9** 345–51
[6] Featherstone J D B and Fried D 2001 Fundamental interaction of lasers with dental hard tissues *Med. Laser Appl.* **16** 181–94
[7] Beltrano J J, Torrisi L, Campagna E, Rapisarda E, Finocchiaro I and Olivi G 2008 Er,Cr:YSGG pulsed laser applied to medical dentistry *Eff. Defects Solids* **163** 331–8
[8] Featherstone J D B and Nelson D G A 1987 Laser effects on dental hard tissues *Adv. Dent. Res.* **1** 21–26
[9] Shinkai K, Suzuki M and Suzuki S 2020 Effects of intensity and frequency of erbium, chromium:yttrium-scandium-gallium-garnet (Er,Cr:YSGG) laser irradiation on tooth ablation *Laser Dent. Sci.* **4** 123–9

[10] Oho T and Morioka T 1990 A possible mechanism of acquired acid resistance of human dental enamel by laser irradiation *Caries Res.* **24** 86–92

[11] Fowler B O and Kuroda S 1986 Changes in heated and in laser-irradiated human tooth enamel and their probable effects on solubility *Calcif. Tissue Int.* **38** 197–208

[12] Morioka T, Tagomori S, Oho T and Clin J 1991 Acid resistance of lased human enamel with Er:YAG laser *Laser Med. Surg.* **9** 215–7

[13] Cecchini R C M, Zezell D M, Oliveira E, Freitas P M and Eduardo C P 2005 Effect of Er:YAG laser on enamel acid resistance: morphological and atomic spectrometry analysis *Lasers Surg. Med.* **37** 366–72

[14] Liu J F, Liu Y, Stephen H C Y and Dent J 2006 Optimal Er:YAG laser energy for preventing enamel demineralization *J. Dent.* **31** 62–66

[15] Sognnaes R F, Stern R H and Calif J S 1965 The effects on resistance of human dental enamel to demineralization *in vitro Dent. Assoc.* **33** 328–9

[16] Featherstone J D B 2000 Caries detection and prevention with laser energy *Dent. Clin. North Am.* **44** 955–69

[17] Rabelo J S, Ana P A, Benetti C, Valério M E G and Zezell D M 2010 Changes in dental enamel oven-heated or irradiated with Er,Cr:YSGG laser. analysis by FTIR *Laser Phys.* **20** 1–5

[18] Marraccini T M, Bachmann L, Wigdor H A, Walsh Jr J T Jr, Stabholtz A and Zezell D M 2005 Morphological evaluation of enamel and dentin irradiated with 9.6 μm and 2.94 μm Er:YAG lasers *Laser Phys. Lett.* **2** 551–5

[19] Lizarelli R F Z, Costa M M, Carvalho Filho E, Nunes F D and Bagnato V S 2008 Selective ablation of dental enamel and dentin using femtosecond laser pulses *Laser Phys. Lett.* **5** 63–69

[20] Marraccini T M, Bachmann L, Wigdor H A, Walsh Jr J T Jr, Turbino M L, Stabholtz A and Zezell D M 2005 Enamel and dentin irradiation with 9.6 μm CO_2 and 2.94 μm Er:YAG lasers: bond strength evaluation *Laser Phys. Lett.* **3** 96–101

[21] Bakhmutov D, Gonchukov S, Kharchenko O, Voytenok O and Zubov B 2008 *Laser Phys. Lett.* **5** 375–8

[22] Suemori T, Kato J, Nakazawa T, Akashi G and Hirai Y 2008 A new non-vital tooth bleaching method using titanium dioxide and 3.5% hydrogen peroxide with a 405-nm diode laser or a halogen lamp *Laser Phys. Lett.* **5** 454–9

[23] LeGeros R Z 1999 Monographs in oral science vol 15

[24] Fleet M E and Liu X Y 2005 Local structure of channel ions in carbonate apatite *Biomaterials* **26** 7548–54

[25] McGraw-Hill 2004 *McGraw-Hill, Encyclopedia of Science and Technology* 5th edn

[26] White T, Ferraris C, Kim J and Madhavi S 2005 Apatite—an adaptative framework structure *Rev. Mineral. Geochem.* **57** 307–401

[27] Wilson R M, Elliot J C and Dowker S E P 1999 Rietveld refinement of the crystallographic structure of human dental enamel apatites *Am. Mineral.* **84** 1406–14

[28] Elliot J C, Wilson R M and Dowker S E P 2002 *Apatite Structures* (JCPDS-International Center for Diffraction Data) vol 45

[29] Ana P A, Bachmann L and Zezell D M 2006 Laser effects on enamel for caries prevention *Laser Phys.* **16** 865

[30] Ana P A, Blay A, Miyakawa W and Zezell D M 2007 Thermal analysis of teeth irradiated with Er,Cr:YSGG at low fluences *Laser Phys. Lett.* **4** 827–34

[31] de Andrade L E H, Pelino J E P, Lizarelli R F Z, Bagnato V S and de Oliveira Jr O B Jr 2007 Enamel caries resistance accidentally irradiated by the Nd:YAG laser *Laser Phys. Lett.* **4** 157–62

[32] Bachmann L, Rosa K, da Ana P A, Zezell D M, Craievich A F and Kellermann G 2009 Crystalline structure of human enamel irradiated with Er,Cr:YSGG laser *Laser Phys. Lett.* **6** 159–62

[33] Bachmann L, Craievich A F and Zezell D M 2004 Crystalline structure of dental enamel after Ho:YLF laser irradiation *Arch. Oral Biol.* **49** 923–9

[34] Meister A C, Ioana R S, Franzen R, Hering P and Gutknecht N 2002 *Lasers Med. Sci.* **17** 246–305

[35] Apel C, Meister J, Ioana R S and Gutknecht N 2002 The ablation threshold of Er:YAG and Er:YSGG laser radiation in dental enamel *Lasers Med. Sci.* **17** 246–52

[36] Belikov A V, Erofeev A V, Shumilin V V and Tkachuk A M 1993 Comparative study of the 3 μm laser action on different hard tissue samples using free running pulsed Er-doped YAG, YSGG, YAP, and YLF lasers *Proc. SPIE* **2080** 60–67

[37] Young R A 1996 The Rietveld method *International Union of Crystallography* (Oxford University Press)

[38] Larson A C and Von Dreele R B 2004 General structure analysis system (GSAS) *Los Alamos National Laboratory Report LAUR* pp 86–748

[39] Haberko K, Bucko M M, Brzezinska-Miecznik J, Kaberko M, Mozgawa W, Panz T, Pyda A and Zarebski J 2006 Natural hydroxyapatite-its behavior during heat treatment *J. Eur. Ceram. Soc.* **26** 537–42

[40] Shih W, Wang J, Wang M and Hon M 2006 A study on the phase transformation of the nanosized hydroxyapatite synthesized by hydrolysis using in situ high temperature x-ray diffraction *Mater. Sci. Eng.* C **26** 1434–8

[41] Pattanayak D K, Dash R, Prasad R C and Rama Mohan T R 2007 Synthesis and sintered properties evaluation of calcium phosphate ceramics *Mater. Sci. Eng.* C **27** 684–90

[42] Hatim Z, Michrafy A, Elassfouri M and Abida F 2009 Stoichiometry and particle morphology effects on the aptitude to compaction of apatitic structure powders *Powder Technol.* **190** 210–4

[43] Tang R, Wang L and Nancoll G H 2004 Size-effects in the dissolution of hydroxyapatite: an understanding of biological demineralization *J. Mater. Chem.* **14** 2341–6

[44] Cai Y and Tang R 2008 Calcium phosphate nanoparticles in biomineralization and biomaterials *J. Mater. Chem.* **18** 3775–87

[45] Tsuchida T, Kubo J, Yoshioka T, Sakuma S, Takeguchi T and Ueda W 2008 Reaction of ethanol over hydroxyapatite affected by Ca/P ratio of catalyst *J. Catal.* **259** 183–9

[46] Liu H, Yazici H, Ergun C, Webster T J and Bermek H 2008 Na *in vitro* evaluation of the Ca/P ratio for the cytocompatibility of nano-to-micron particulate calcium phosphate for bone regeneration *Acta Biomater.* **4** 1472–9

[47] Park Y M, Ryu S C, Yoon S Y, Stevens R and Park H C 2008 Preparation of whisker-shaped hydroxyapatite/β-tricalcium phosphate composite *Mater. Chem. Phys.* **109** 440–7

[48] Klopcic S B, Kovac J and Kosmac T 2007 Apatite-forming ability of alumina and zirconia ceramics in a supersaturated Ca/P solution *Biomol. Eng.* **24** 467–71

[49] Lagergren E S, Colbert J C and MacDonald B S 2003 Standard reference material 2910: calcium hydroxyapatite (National Institute of Standards e Technology)

[50] Secilmis A, Usumes A, Usumez S and Berk G 2008 Evaluation of mineral content of dentin prepared by erbium, chromium: yttrium scandium gallium garnet laser *Lasers Med. Sci.* **23** 421–5

[51] Erkmen Almaz M, Ulusoy N B, Akbay Oba A, Erdem Ü and Doğan M 2021 Thermal, morphological, and spectral changes after Er, Cr:YSGG laser irradiation at low fluences on primary teeth for caries prevention *Microsc. Res. Tech.* **84** 150–9

[52] Alkhudhairy F, Naseem M, Bin-Shuwaish M and Vohra F 2018 Efficacy of Er Cr: YSGG laser therapy at different frequencies and power levels on the bond integrity of composite to bleached enamel *Photodiagnosis Photodyn. Ther.* **22** 34–38

[53] Ulusoy N, Akbay Oba A and Cehreli Z 2020 Effect of Er,Cr:YSGG laser on the prevention of primary and permanent teeth enamel demineralization: SEM and EDS evaluation *Photobiomodulation Photomed. Laser Surg.* **38** 308–15

[54] Benetti C, Ana P A, Bachmann L and Zezell D M 2015 Mid-infrared spectroscopy analysis of the effects of erbium, chromium: yttrium-scandium-gallium-garnet (Er,Cr:YSGG) laser irradiation on bone mineral and organic components *Appl. Spectrosc.* **69** 1496–504